

**SPECIAL ISSUE ARTICLE**

Solid-state synthesis of cyclo LD-diphenylalanine: A chiral phase built from achiral subunits

Ariel Pérez-Mellor | Katia Le Barbu-Debus | Anne Zehnacker

Institut des Sciences Moléculaires d'Orsay (ISMO), CNRS, University Paris-Sud, Université Paris-Saclay, Orsay, France

Correspondence

Ariel Pérez-Mellor and Anne Zehnacker, Institut des Sciences Moléculaires d'Orsay (ISMO), CNRS, University Paris-Sud, Université Paris-Saclay, F-91405 Orsay, France.

Email: ariel-francis.perez-mellor@u-psud.fr; anne.zehnacker-rentien@u-psud.fr

Abstract

The solid-state structure of LL/DD or LD/DL diphenylalanine diluted in KBr pellets is studied by infrared (IR) absorption and vibrational circular dichroism (VCD) spectroscopy. The structure depends on the absolute configuration of the residues. The natural LL diphenylalanine exists as a mixture of neutral and zwitterionic structures, depending on the humidity of the sample, while mostly the zwitterion is observed for LD diphenylalanine whatever the experimental conditions. The system undergoes spontaneous cyclization upon heating at 125°C, resulting to the formation of a diketopiperazine (DKP) dipeptide as the only product. The reaction is faster for LD than for LL diphenylalanine. As expected, LL and DD diphenylalanine react to form the LL and DD enantiomers of cyclo diphenylalanine. Interestingly, the DKP dipeptides formed from the LD or DL diphenylalanine show unexpected optical activity, with opposite VCD spectra for the products formed from the LD and DL reagents. This is explained in terms of chirality synchronization between the monomers within the crystal, which retain the symmetry of the reagent, resulting to the formation of a new chiral phase made from transiently chiral molecules.

KEYWORDS

chirality synchronization, diketopiperazine (DKP), peptides, vibrational circular dichroism (VCD), vibrational spectroscopy

1 | INTRODUCTION

Oligopeptides are important building blocks for the synthesis of supramolecular structures due to their self-assembly capabilities.^{1–8} The wealth of nanostructures formed opens a wide range of applications in the field of biosensors, organic semiconductors, and drug delivery.^{9–12} In particular, nanostructures formed from the Alzheimer's β -amyloid linear dipeptide diphenylalanine show a large degree of polymorphism. They have been extensively studied theoretically^{13–18} and experimentally.^{19,20} The balance between dispersive interactions among aromatic substituents and electrostatic

interactions between the polar termini results in the formation of very stiff nanotubes consisting of a cyclic structure containing six molecules. The packing of these rings determines a supramolecular structure with chirality defined by that of the monomer, namely, a left-handed helix for the natural LL diphenylalanine. The crystallographic study of these nanotubes suggests that their structure is the same as that of the single-crystal structure. Water has been suggested to play a role in the stabilization process.¹⁵ The molecules are indeed in their zwitterion form and are bound by strong interactions between the COO^- and NH_3^+ termini, the zwitterions being stabilized in aqueous environments.²¹ The benzene

rings are in a T-shape configuration. Such a geometry is reminiscent of that observed in diphenylalanine or capped diphenylalanine isolated in the gas phase under supersonic jet conditions.^{22,23}

Diphenylalanine, like other dipeptides built on aromatic residues, spontaneously undergoes intramolecular peptide bond formation.^{5,24-27} The reaction product is a cyclic dipeptide called diketopiperazine (DKP). In particular, diphenylalanine nanotubes thermally cyclize to DKP structures.²⁸ DKP peptides find applications as antivirals, antiparasitics, anticancer agents,²⁹⁻³¹ or as catalysts.^{32,33}

Unlike linear dipeptides, DKP-containing dipeptides do not possess a terminal charged group, and their crystal structure mainly involves NH ... OC hydrogen bonding interactions. The cyclo diphenylalanine crystal consists indeed of ladder-like structures bridged by a double NH ... O=C hydrogen bond.³⁴ The subunit of the crystal has a structure identical to that observed in the gas phase, with one aromatic ring folded over the DKP ring in a flagpole position and the other extended.²² Fourier transform infrared (FTIR) and vibrational circular dichroism (VCD) spectroscopy of cyclo diphenylalanine powder in KBr pellets indicate that the system can be described as a dimer bridged by the same double hydrogen bond interaction as observed in the single crystal.³⁵

Most studies conducted so far are devoted to dipeptides of natural absolute configuration L. The influence of the L or D absolute configuration of the residues on the self-assembly propensity of oligopeptides has been studied by electronic circular dichroism.³⁶ Tripeptides based on L or D phenylalanine have been studied by circular vibrational dichroism, and γ -turn nanostructures have been observed for L-Phe-L-Phe-D-Phe.³⁷ We have recently compared the structure of jet-cooled diphenylalanine, denoted as LL hereafter, and cyclo diphenylalanine, denoted as c-LL, to that of their diastereomer LD diphenylalanine (LD) and cyclo LD diphenylalanine (c-LD). Conformer-selective vibrational spectroscopy compared with quantum chemical calculations indicates that the structural differences between the two diastereomers are small.^{22,38,39} c-LL and c-LD both show a folded-extended conformation, with one of the aromatic ring folded over the dipeptide frame and the other one extended outwards. c-LL and c-LD differ by the strength and the nature of CH ... π or NH ... π interactions. The most stable structure of linear LL and LD diphenylalanine both involve an extended structure of the peptide chain, with free NH₂ and COOH groups at the termini. A bifurcated hydrogen bond takes place from the amide NH as a donor to both the acid CO and the NH₂ group. LL and LD mostly differ by the position of the aromatic rings. Similar minor differences were

observed for the protonated systems or the alkali-core complexes isolated in an ion trap.⁴⁰⁻⁴²

In this work, we extend our FTIR and VCD studies on c-LL to its linear dipeptide precursor LL, as well as their diastereomers LD and c-LD. (Figure 1).

This work aims at comparing the solid-state structure of the powder of each diastereomer cyclo diphenylalanine and linear diphenylalanine. The presence of aromatic rings may influence the binding pattern by competing with the hydrogen-bond formation, and we will compare the IR spectra of c-LD and c-LL at the light of this competition. While the stable form of most amino acids in the solid is a zwitterion, the oligopeptides can be either neutral or zwitterion, depending on the length of the peptide, the nature of the residue, and the environment, in particular presence of water. In what follows, we will also get information on the competition between neutral and zwitterion forms of LL and LD from their vibrational spectroscopy.

The second part of this work is devoted to the in situ synthesis of cyclo diphenylalanine by heating the KBr pellet and to the study of the cyclo diphenylalanine crystal obtained thereby. In solution, the reaction seems to proceed in the neutral dipeptide and not in the zwitterion.^{43,44} The synthesis of DKP on a solid support has also been described.⁴⁵ However, despite the existence of numerous studies on dipeptide cyclization, the reaction has not been studied yet in KBr pellets.

2 | MATERIALS AND METHODS

2.1 | Sample preparation

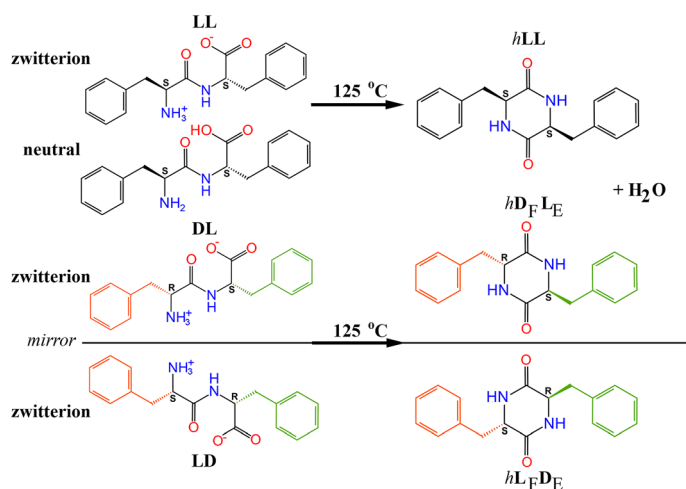


FIGURE 1 Systems under study and thermal reaction scheme. The colored residues simulate the asymmetric positions of the benzene rings (see text) [Colour figure can be viewed at wileyonlinelibrary.com]

The dipeptides (98% purity) were purchased from GeneCust-Luxembourg and Novopep Limited (Shanghai, China) and used without further purification. KBr pellets of the samples were prepared in the following way: first, 10 mg of the studied molecules diluted with 3.5 g of KBr were carefully grinded in a mixer mill (MM 400 Retsch) at 20 Hz during 1 h. This procedure avoids the formation of large crystals (>5 μm) that could induce birefringence. The pellets were then made by pressing 150 mg of this mixture up to 7 tons using a manual hydraulic press. Finally, the pellets were smoothly heated up to 80°C for 24 h to eliminate most of the water.

2.2 | Mass spectrum

A mass spectrum was recorded for each pellet after the thermal reaction, to check the nature of the products. The pellets were dissolved into a mixture of methanol and water (50:50) to form a 1-mM stock solution. The pH of the solution was neutral. It was shown in our previous study that the LL or LD linear diphenyl alanine is neutral and not zwitterionic in the gas phase.⁴⁰ The potassium core molecular complexes were generated by electro-spraying a 100- μM solution obtained by diluting the stock solution. The mass spectrum was recorded in a 7 T Fourier-transform ion cyclotron resonance (FTICR) hybrid mass spectrometer (Bruker, Apex Qe) at the mass spectrometry platform Spectrométrie de Masse, Analyse, et Spectroscopie (SMAS) of the Laboratoire de Chimie Physique (University Paris-Sud).

2.3 | Attenuated total reflection-FTIR spectroscopy

The attenuated total reflection (ATR)-FTIR spectra were performed using the conventional ALPHA II FTIR spectrometer from Bruker through the single reflection Eco-ATR module. All the data were collected with a resolution of 2 cm^{-1} .

2.3.1 | FTIR and VCD spectroscopy

The IR and the VCD spectra of the pellets were recorded using an FTIR spectrometer (Vertex 70 Bruker) equipped with a VCD module (PMA 50 Bruker) consisting of a photoelastic modulator (PEM) and a fast-acquisition dual channel. The IR spectrum was measured over the whole 800 to 3700 cm^{-1} range at a 2- cm^{-1} resolution while the VCD spectrum was

obtained only in the 800 to 1800 cm^{-1} region. The alignment of the spectrometer was controlled by monitoring the mirror-image relation between the VCD spectra of the two enantiomers of camphor (0.3 M in CCl_4). The possible artefacts due to the KBr pellets birefringence were corrected by following the procedure proposed by Merten et al derived from that introduced by Buffeteau et al.^{46,47} Briefly, it consists in rotating the sample in the plane perpendicular to the light propagation axis for each side (front F or back B) at 0° and 90°. Therefore, each VCD spectrum is composed of the average between the four spectra recorded at the different crystal sample positions. Each spectrum shown hereafter corresponds to 4-h acquisition time, ie, 1 h per orientation.

2.4 | Solid-state synthesis

Spontaneous cyclization reaction was obtained by heating the LL and LD pellets to a temperature of 125°C for increasing times.²⁷ The reproducibility of the experiment was checked by repeating the procedure on three different pellets, for LL and LD, and verifying that the results are identical. The reaction was monitored by recording the IR spectra as a function of time. The spectra were taken before putting the pellets into the oven (time zero) then after 1, 4, 9, and 21 h in the oven. The reaction was considered to be completed when the IR spectrum did not evolve in time anymore. Then, a VCD spectrum was recorded as described above.

3 | RESULTS AND DISCUSSION

3.1 | IR spectroscopy of solid-state c-LL and c-LD

Figure 2 compares the IR absorption spectrum of c-LL and c-LD diluted in KBr with the ATR spectrum of the pure powder, in the amide I and II regions. The similitude between the two spectra confirms that the KBr pellet and the pure solid are constituted of powder of identical nature, namely, microcrystals. The diastereomers especially differ in the amide I region: as reported before, c-LL shows a doublet at 1663 to 1677 cm^{-1} , which contrasts to the single broadened band at 1677 cm^{-1} in c-LD.³⁵ The doublet observed for the ν (CO) stretch of c-LL was assigned to bound and free CO groups within dimers involving a double NH..OC bond, an assignment confirmed by VCD spectra.³⁵ The single band observed in c-LD is characteristic of free CO groups. It is therefore

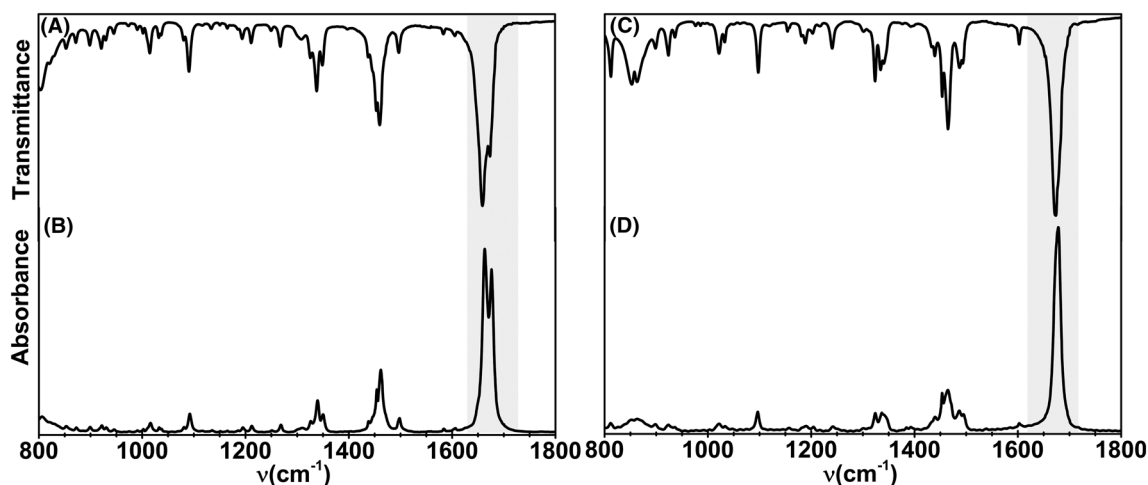


FIGURE 2 Attenuated total reflection (ATR) Fourier transform infrared (FTIR) spectrum of the pure powder of (A) c-LL and (C) c-LD. FTIR absorption of the KBr pellet of (B) c-LL and (D) c-LD

likely that the crystal cohesion is mainly due to dispersion in c-LD. As expected for the symmetrical c-LD, no VCD signal was observed.

3.2 | IR spectroscopy of solid-state LL and LD

Figure 3 compares the IR absorption of LL and LD in a KBr pellet with the ATR spectrum of the pure powder, in the fingerprint region.²⁷ The ATR and IR absorption

spectra are very similar, pointing at the polycrystalline nature of the samples. The ATR spectrum shown here strongly differs from that reported for the self-assembled nanotubes, which contain three well-defined transitions at 1256, 1389, and 1555 cm^{-1} . These transitions are not observed here. Moreover, the bands 1143 (A), 1205 (B), (H), and 1732 cm^{-1} (I) present in the ATR spectrum reported here are absent in that of the nanostructures.¹⁹ These results allow us to rule out the existence of supra-molecular nanostructures in the sample studied here. The IR absorption is congested and shows bands due to

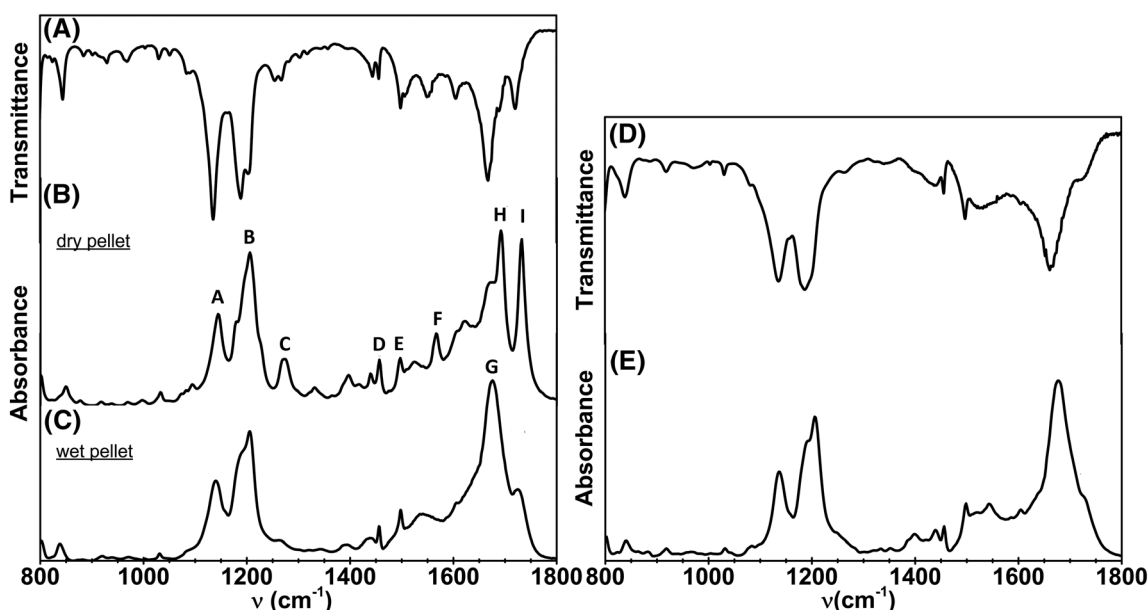


FIGURE 3 Fourier transform infrared (FTIR) (top) and vibrational circular dichroism (VCD) (bottom) spectra in the fingerprint region of (A) LL and (B) LD

both neutral and zwitterion forms of the dipeptides. This is especially apparent for the ν (CO) stretch, which dominates the fingerprint region. First, two narrow features are observed at 1732 and 1691 cm^{-1} . The former is the ν (CO) stretch of the carboxylic acid COOH and the latter the ν (CO) stretch of the peptide bond. Second, an intense band is observed at 1676 cm^{-1} (G). It is assigned to the ν (CO) stretch of the carboxylate anion COO^- of the zwitterion.⁴⁸ The ratio between the neutral vs zwitterion contributions depends on the water content of the pellet and on the relative absolute configuration of the residues. Pellets left at ambient conditions are strongly hydrated, as attested by the broad bands at ~ 3440 and ~ 1630 cm^{-1} due to ν_3 and ν_2 of water. In these conditions, the zwitterion dominates, for both LL and LD samples, which show almost identical spectra. For pellets kept 12 h at 80°C, the neutral and zwitterion contributions are of the same order of magnitude for LL. No effects of humidity are observed for LD that always shows a dominant contribution of the zwitterion.

Several transitions appear in the NH bend region at 1456 (D), 1498 (E), and 1566 cm^{-1} (F). Apart from the latter, which is observed in dry LL only and is therefore assigned to the neutral dipeptides, the other bands are of limited intensity. They are not structure dependent nor are the intense aromatic and aliphatic CH bending modes at 1060 to 1280 cm^{-1} . These bands are not very sensitive to the neutral or zwitterionic nature of the molecule, apart from that at 1271 cm^{-1} (C), which is characteristic of the neutral form. They are not sensitive either to the relative absolute configuration. Therefore, we will not consider them further.

The hydride stretch region, shown in Figure S1 of the electronic supporting information (ESI), is characterized

by a broadband absorption between 2400 and 2800 cm^{-1} , attributed to a zwitterion, like observed in alanine diluted in KBr pellets.⁴⁸

Sharper bands at 3302 and 3173 cm^{-1} are assigned to the amide ν (NH) stretches.

3.3 | Vibrational circular dichroism of solid-state LL and LD

Figure 4 reports the VCD spectra of LL and LD diluted in KBr, as well as that of their enantiomers. A good mirror image relation is obtained between the spectra of enantiomers. Broad features in the IR absorption spectrum appear as multiplets in the VCD spectrum, which indicates that they correspond to superimposed IR transitions. The bands due to the neutral species at 1271, 1566, and 1732 cm^{-1} are relatively intense in the VCD spectrum of LL. They all show a bisignate pattern. The 1060 to 1280 cm^{-1} region also shows strong VCD activity.

LD shows VCD intensities about seven times weaker than LL. The 1060 to 1280 cm^{-1} is still the most active one, as it was in LL. The 1600 to 1800 cm^{-1} region is more complex than in LL.

The VCD spectra of c-LL and c-LD have been reported before. As expected for a symmetrical compound, the spectrum of c-LD shows no activity.

3.4 | Formation of cyclo diphenylalanine by a thermal reaction

Both LD and LL IR absorption spectra evolve with heating time, which indicates their transformation into

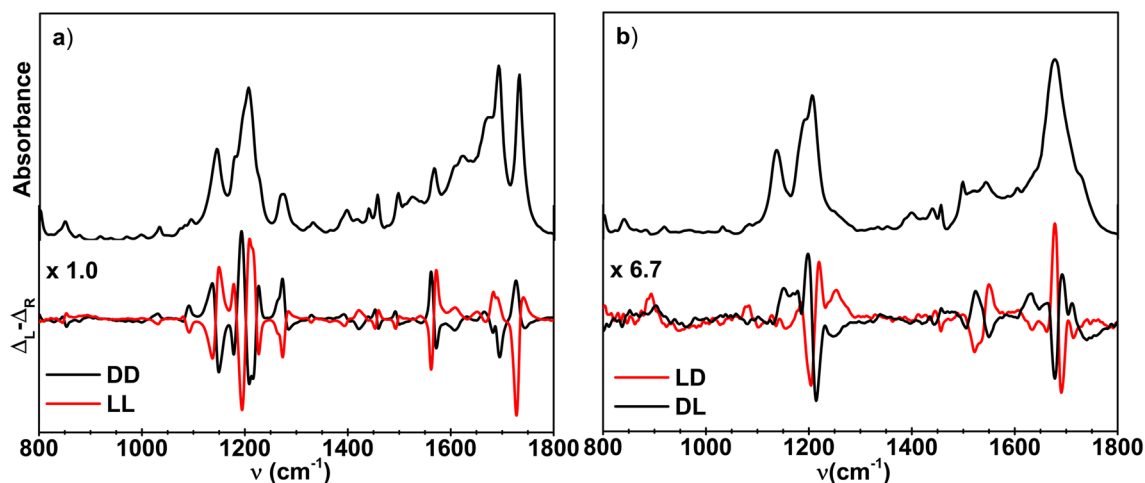


FIGURE 4 (A) Attenuated total reflection (ATR) Fourier transform infrared (FTIR) spectrum of the pure LL powder in the 800 to 1800 cm^{-1} region. (B) FTIR spectrum of LL diluted in a KBr pellet (dry pellet) (C) same for a water-containing pellets. (D) ATR-FTIR spectrum of the pure LD powder in the 800 to 1800 cm^{-1} region. (E) FTIR spectrum of LD diluted in a KBr pellet [Colour figure can be viewed at wileyonlinelibrary.com]

a product referred to as *hLL* and *hLD*, where *h* stands for “heated.” The kinetics are identical for the three samples tested for a given diastereomer, but the thermal reaction is faster for LD than LL. The fact that the difference spectra (Figure S2 of the ESI) show bands that continuously increase while others steadily decrease with time suggests the absence of intermediate structures, at least on a measurable time scale, in the reactive process.

After completion of the thermal reaction, the mass spectrum recorded for electrosprayed solutions made from each pellet indicates the presence of cyclo diphenylalanine, as well as the complete disappearance of the parent linear dipeptide (see Figure S3 of the ESI). No peak corresponding to CO₂ loss from the parent is observed, which indicates that DKP formation is the only product. This is in contrast to the same reaction involving phenylalanine on silica, for which CO₂ loss was also observed.⁴⁹ The mass spectra therefore suggest that *hLL* and *hLD* indeed are *c-LL* and *c-LD*.

The comparison between IR absorption spectra of the thermal reaction products, namely, *hLL* and *hLD*, and *c-LL* and *c-LD* confirms this hypothesis (Figure 5). The IR spectra are very similar indeed in terms of shape and position of the bands. However, the band assigned to the bound ν (CO) stretch is shifted down by 2 cm⁻¹ in *hLL* relative to *c-LL*. *c-LD* and *hLD* also show small differences in that region. In *c-LD*, the band shows an asymmetry (frequency separation between the two free ν (CO) stretches) of 7 cm⁻¹ while in *hLD*, it is 11 cm⁻¹. These minor differences might reflect a difference in crystal packing.

3.5 | Formation of a chiral phase

3.5.1 | Achiral cyclo LD diphenylalanine

c-DL and *c-LD* purchased from the supplier exhibit identical IR absorption and do not possess any VCD activity. The lack of optical activity can be due to two reasons. First, *c-LD* could be a C_i molecule, devoid of chirality due to the presence of a center of symmetry.³⁹ In this case, *c-LD* and *c-DL* are identical non-chiral molecules. However, laser spectroscopy combined with quantum chemical calculations indicates that the C_i structure is a transition state and that the most stable form in the gas phase is a nonsymmetrical C₁ structure, with nonequivalent phenyl groups. One phenyl is indeed folded over the DKP ring while the other one is extended outwards. In what follows, we will denote the phenyl position by a subscript F for folded and E for extended. *c-LD* (*c-DL*) is chiral because *c-L_FD_E* (*c-D_FL_E*) is the mirror image of *c-L_ED_F* (*c-D_EL_F*). As *c-L_FD_E* and *c-D_EL_F* are identical, we are left with two enantiomers, *c-L_FD_E* and *c-L_ED_F*. The interconversion between them proceeds through large-amplitude motions and involves low barriers. As a result, *c-LD* is a racemic mixture of two easily converting enantiomers, which explains its lack of VCD activity.

3.5.2 | Formation of chiral cyclo LL and DD diphenylalanine

The VCD spectrum of *hLL* is the mirror image of that of *hDD*. It is very similar to that of *c-LL*, notwithstanding

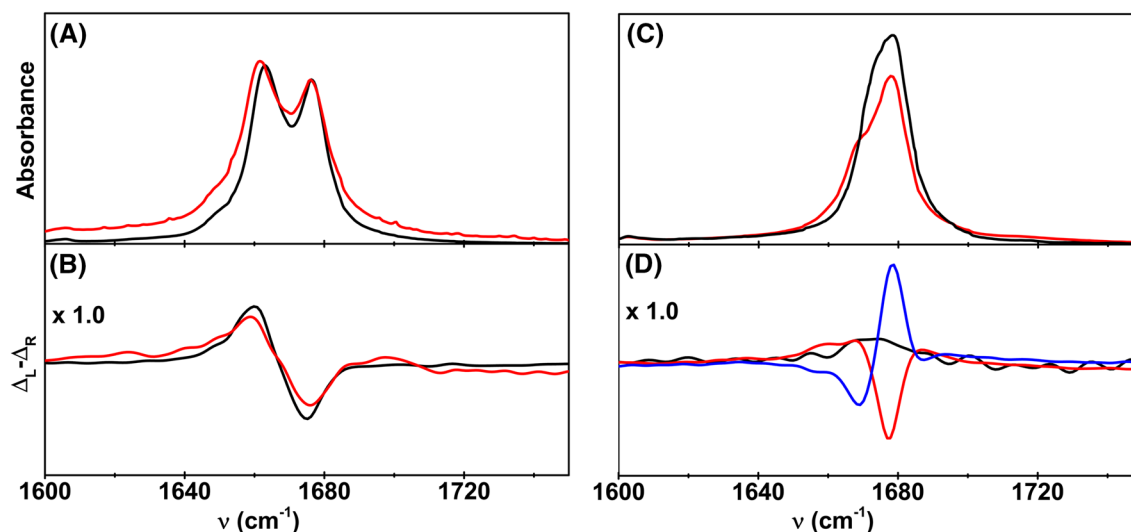


FIGURE 5 Comparison between the spectra of the reaction products *hLL* (red line) and *c-LL* (black line) in the region of the ν (CO) stretch: (A) infrared (IR) absorption in absorbance (A) units and (B) vibrational circular dichroism (VCD) spectra. Same comparison for the reaction products *hLD* (red line), *hDL* (blue line) and *c-LD* (black line): (C) IR absorption and (D) VCD spectra [Colour figure can be viewed at wileyonlinelibrary.com]

the small broadening at the low-energy side, which was already apparent in the IR absorption. Similarly, the VCD spectrum of *h*DD compares well with that of *c*-DD. The VCD spectra, therefore, confirm the other experimental findings, namely, the mass spectra (MS) and FTIR results, that *h*LL is identical to *c*-LL and *h*DD to *c*-DD. As peptide bond formation preserves the absolute configuration of the amino acid chiral centers, VCD activity of the products is expected.

3.5.3 | Formation of chiral cyclo LD and DL diphenylalanine

VCD activity in *h*LD is more surprising. The fact that *h*LD shows optical activity, in contrast to *c*-LD, suggests that the crystal is chiral. Moreover, the VCD spectra of *h*LD and *h*DL show specular relation. Therefore, enantiomers are formed when starting from LD or DL. We can discuss these surprising results at the light of what is known on chiral supramolecular objects. These objects can first form from completely achiral subunits assembled in a chiral manner.⁵⁰ The formed system can be a conglomerate, in the absence of perturbation⁵¹ or can be driven into a given chirality by a chiral influence. This is the case for foldamers built from achiral monomers, the helicity of which is determined by the absolute configuration of chiral tartrate gemini.⁵² Second, it can form from non-permanent chiral subunits that synchronize their chirality.^{53,54} This is observed for 2-propyl-1-H-benzimidazole in the solid state.⁵⁵ The molecular subunit is transiently chiral, although free rotation around a single bond allows fast interconversion between the enantiomers in solution. Still, the molecule crystallizes as a chiral crystal endowed with a chiroptical response. This is an example of chirality synchronization, a phenomenon that has been observed also under isolated conditions.⁵⁶ ⁵⁷ Surprisingly, always the same enantiomers of the 2-propyl-1-H-benzimidazole crystal is found whatever the experimental conditions. Our results contrast to the latter as enantiomeric crystals are formed when reacting enantiomeric reagents. This can be explained by considering the possible cyclization mechanism in the KBr pellet, leading to the DKP formation from the linear dipeptide. The proposed mechanism in solution involves neutral dipeptide.⁴³ The first step is the isomerization of the amide, from *trans* to *cis* geometry of the peptide bond,⁵⁸ as confirmed by theoretical studies.^{59,60} This allows nucleophilic addition of the amino group to the carbonyl carbon atom and then the loss of water to form the DKP ring. It was also noticed that the dipeptide with alternate absolute configuration shows larger

cyclization propensity due to steric effects; the LD configuration of the DKP involves indeed substituents on opposite sides of the DKP ring.⁵⁸ This is in line with the experimental findings described here that LD cyclizes more rapidly than LL.

3.5.4 | Symmetry consideration

A possible interpretation of the observed effect rests upon the symmetry of the reagent. Although both residues are indiscernible in the product, they are non-symmetrical in the reagent because one of them is on the C terminus and the other one on the N terminus. The most stable calculated structures of jet-cooled LL and LD, to which the experimentally observed species were assigned, involve a bifurcated hydrogen bond with the amide NH interacting with both the NH₂ terminus and the acid CO, see Figure 6. The phenyl rings are in a T-shape arrangement.²² The isomerization of the amide may involve rotation around the amide bond. If the reaction proceeds in solution or on resin, the amide rotation is accompanied by free rotation of the benzyl substituents. As a result, the chiral centers lose the memory of their origin, in other words, whether they were located on the N or C terminus. A racemic mixture of *c*-L_FD_E and *c*-L_ED_F is obtained resulting in zero VCD signal. If the reaction is conducted in the KBr pellets, the phenyl rotation is not free in the solid and each phenyl keeps a selected orientation depending on the terminus it belongs to. We will use as an example the most stable form of DL where D is the N terminus (see Figure 6). In this structure, the phenyl on the D residue is folded over the peptide backbone and the L is directed outside. Rotating the amide bond and conducting the reaction without rotating the benzyl substituents results in *c*-D_FL_E. Conversely, starting from the same geometry for LD results to *c*-L_FD_E, which is enantiomer to *c*-D_FL_E. This reaction illustrates well the Curie principle postulated in 1894 saying that “the symmetries of the causes are to be found in the effects.”

The comparison between the experimental VCD spectra, in the amide I region, and those simulated in the gas-phase for the *c*-L_FD_E and *c*-D_FL_E enantiomers is shown in Figure 7. The whole spectrum is shown in Figure S4. The calculated spectrum corresponds to the previously published B conformer, which is the second most stable conformer in the gas phase.²² Briefly, the spectrum was calculated in the frame of the density functional theory at the B3LYP/6-311++g(d,p) level, including the D3 empirical dispersion term, using the Gaussian 09 software.⁶¹ The calculated frequencies were empirically scaled by 0.952 to make the experimental

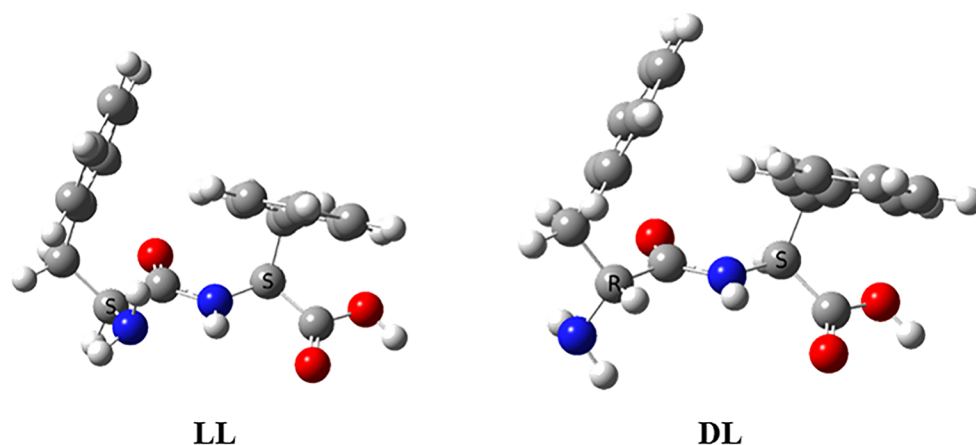


FIGURE 6 Most stable geometry of LL and DL in the gas phase [Colour figure can be viewed at wileyonlinelibrary.com]

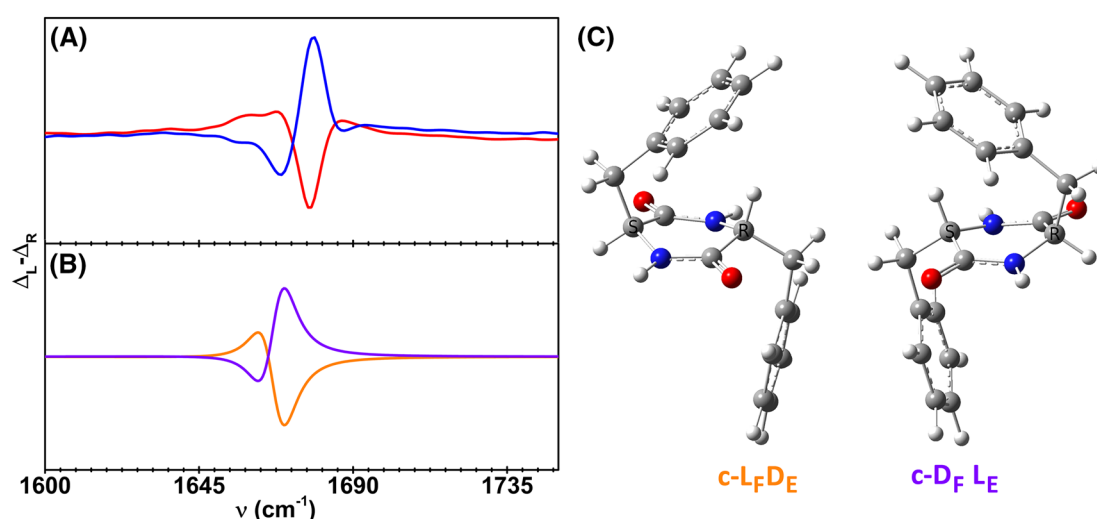


FIGURE 7 A, Experimental vibrational circular dichroism (VCD) spectrum of hLD (red line) and hDL (blue line). B, Simulated VCD spectrum of $c\text{-L}_F\text{D}_E$ (orange line) and $c\text{-D}_F\text{L}_E$ (violet line). C, Corresponding calculated structures [Colour figure can be viewed at wileyonlinelibrary.com]

and calculated ν (CO) match. This unusually large scaling factor accounts not only for anharmonicity and basis set incompleteness but also for the fact that we use the spectrum of a monomer to reproduce that of a crystal. Despite this approach being justified by the fact that the crystal is a dispersion-driven structure, deprived of NH ... O hydrogen bonds, this is still a crude approximation, which explains the deficiencies of the calculated spectrum, in particular the overestimated gap between the ν (CO) and β (NH) bands. However, a good agreement is obtained between experiment and calculation in the ν (CO) region, and none of the other calculated conformers of $c\text{-LD}$ accounts for the experimental spectrum.³⁵ This argument reinforces our conclusion concerning the formation of a chiral phase resulting from chirality synchronization between transiently chiral subunits similar to that shown in Figure 7.

4 | CONCLUSION

The comparison between ATR and IR absorption spectra shows that the pure solid and the sample diluted in KBr pellets have identical structures. $c\text{-LL}$ and $c\text{-LD}$ differ in their packing. While the $c\text{-LL}$ powder is composed of hydrogen-bonded dimers, the cohesion of $c\text{-LD}$ crystals is mainly due to dispersion. IR spectroscopy clearly indicates that the samples of LL and LD linear dipeptides studied here are not composed of nanotubes. LL is composed of a mixture of zwitterion and neutral forms of the peptide, whose relative contributions depend on the water content of the sample. In contrast, LD mainly exists as a zwitterion. In situ synthesis of cyclo diphenylalanine is easily achieved by heating the parent linear dipeptides at a temperature of $\sim 125^\circ\text{C}$. Interestingly, the $c\text{-LD}$ DKP dipeptide formed thereby shows

optical activity. Moreover, the cyclic dipeptides formed from the LD and DL parents are enantiomers and show opposite VCD spectra. This is tentatively explained in terms of chirality synchronization between the monomers within the crystal, which retain the chirality of the reagent. Besides providing information on the structure of the solid, VCD experiments allowed, therefore, evidencing a new chiral phase made from a transiently chiral molecule.

ACKNOWLEDGMENTS

We thank Mr Antoine Béthune and Mr Jérémy Lefèbvre for experimental assistance.

ORCID

Anne Zehnacker  <https://orcid.org/0000-0001-5540-0667>

REFERENCES

- Guo C, Luo Y, Zhou R, Wei G. Triphenylalanine peptides self-assemble into nanospheres and nanorods that are different from the nanovesicles and nanotubes formed by diphenylalanine peptides. *Nanoscale*. 2014;6(5):2800-2811.
- Joshi KB, Verma S. Participation of aromatic side chains in diketopiperazine ensembles. *Tetrahedron Lett*. 2008;49(27):4231-4234.
- Manchineella S, Govindaraju T. Molecular self-assembly of cyclic dipeptide derivatives and their applications. *ChemPlusChem*. 2017;82(1):88-106.
- Jeon J, Shell MS. Self-assembly of cyclo-diphenylalanine peptides in vacuum. *J Phys Chem B*. 2014;118(24):6644-6652.
- Jeziorna A, Stopczyk K, Skorupska E, et al. Cyclic dipeptides as building units of nano- and microdevices: synthesis, properties, and structural studies. *Cryst Growth Des*. 2015;15(10):5138-5148.
- Amaral HR, Kogikoski S, Silva ER, Souza JA, Alves WA. Micro- and nano-sized peptidic assemblies prepared via solid-vapor approach: morphological and spectroscopic aspects. *Mater Chem Phys*. 2012;137(2):628-636.
- Amdursky N, Molotskii M, Gazit E, Rosenman G. Elementary building blocks of self-assembled peptide nanotubes. *J Am Chem Soc*. 2010;132(44):15632-15636.
- Mossou E, Teixeira SCM, Mitchell EP, et al. The self-assembling zwitterionic form of L-phenylalanine at neutral pH. *Acta Crystallogr C*. 2014;70(3):326-331.
- Lee JS, Yoon I, Kim J, Ihee H, Kim B, Park CB. Self-assembly of semiconducting photoluminescent peptide nanowires in the vapor phase. *Angewandte Chemie Int Ed*. 2011;50(5):1164-1167.
- Kogikoski S, Sousa CP, Liberato MS, et al. Multifunctional biosensors based on peptide-polyelectrolyte conjugates. *Phys Chem Chem Phys*. 2016;18(4):3223-3233.
- Silva RF, Araújo DR, Silva ER, Ando RA, Alves WA. L-Diphenylalanine microtubes as a potential drug-delivery system: characterization, release kinetics, and cytotoxicity. *Langmuir*. 2013;29(32):10205-10212.
- Adler-Abramovich L, Reches M, Sedman VL, Allen S, Tandler SJB, Gazit E. Thermal and chemical stability of diphenylalanine peptide nanotubes: implications for Nanotechnology applications. *Langmuir*. 2006;22(3):1313-1320.
- Guo C, Luo Y, Zhou R, Wei G. Probing the self-assembly mechanism of diphenylalanine-based peptide nanovesicles and nanotubes. *ACS Nano*. 2012;6(5):3907-3918.
- Jeon J, Mills CE, Shell MS. Molecular insights into diphenylalanine nanotube assembly: all-atom simulations of oligomerization. *J Phys Chem B*. 2013;117(15):3935-3943.
- Andrade-Filho T, Martins TC, Ferreira FF, Alves WA, Rocha AR. Water-driven stabilization of diphenylalanine nanotube structures. *Theoretic Chem Acc*. 2016;135(8):185.
- Andrade-Filho T, Ferreira FF, Alves WA, Rocha AR. The effects of water molecules on the electronic and structural properties of peptide nanotubes. *Phys Chem Chem Phys*. 2013;15(20):7555-7559.
- Rissanou AN, Georgilis E, Kasotakis E, Mitraki A, Harmandaris V. Effect of solvent on the self-assembly of dialanine and diphenylalanine peptides. *J Phys Chem B*. 2013;117(15):3962-3975.
- Azuri I, Adler-Abramovich L, Gazit E, Hod O, Kronik L. Why are diphenylalanine-based peptide nanostructures so rigid? Insights from first principles calculations. *J Am Chem Soc*. 2014;136(3):963-969.
- Görbitz CH. Nanotube formation by hydrophobic dipeptides. *Chem A Eur J*. 2001;7(23):5153-5159.
- Goerbitz CH. The structure of nanotubes formed by diphenylalanine, the core recognition motif of Alzheimer's beta-amyloid polypeptide. *Chem Commun*. 2006;22:2332-2334.
- Im S, Jang SW, Lee S, Lee Y, Kim B. Arginine zwitterion is more stable than the canonical form when solvated by a water molecule. *J Phys Chem A*. 2008;112(40):9767-9770.
- Perez-Mellor A, Alata I, Lepere V, Zehnacker A. Chirality effects in the structures of jet-cooled bichromophoric dipeptides. *J Molec Spectroscopy*. 2018;349:71-84.
- Gloaguen E, Valdes H, Pagliarulo F, et al. Experimental and theoretical investigation of the aromatic-aromatic interaction in isolated capped dipeptides. *Chem A Eur J*. 2009;14(9):2973-2982.
- Borthwick AD. 2,5-Diketopiperazines: synthesis, reactions, medicinal chemistry, and bioactive natural products. *Chem Rev*. 2012;112(7):3641-3716.
- Basiuk VA, Gromovoy TY. The gas solid-phase 2,5-dioxopiperazine synthesis—cyclization of vaporized dipeptides on silica surface. *Collec Czechoslovak Chem Commun*. 1994;59(2):461-466.
- Ziganshin MA, Safiullina AS, Gerasimov AV, et al. Thermally induced self-assembly and cyclization of l-leucyl-l-leucine in solid state. *J Phys Chem B*. 2017;121(36):8603-8610.
- Ziganshin MA, Gerasimov AV, Ziganshina SA, et al. Thermally induced diphenylalanine cyclization in solid phase. *J Thermal Anal Calorimetry*. 2016;125(2):905-912.
- Jaworska M, Jeziorna A, Drabik E, Potrzebowski MJ. Solid state NMR study of thermal processes in nanoassemblies formed by dipeptides. *J Phys Chem C*. 2012;116(22):12330-12338.
- Sinha S, Srivastava R, De Clereq E, Singh RK. Synthesis and antiviral properties of arabino and ribonucleosides of 1,3-dideazaadenine, 4-nitro-1,3-dideazapurine and

- diketopiperazine. *Nucleosides Nucleotides Nucleic Acids*. 2004; 23(12):1815-1824.
30. Grande F, Garofalo A, Neamati N. Small molecules anti-HIV therapeutics targeting CXCR4. *Curr Pharm Des*. 2008;14(4): 385-404.
31. Walchshofer N, Sarciron ME, Garnier F, Delatour P, Petavy AF, Paris J. Anthelmintic activity of 3,6-dibenzyl-2,5-dioxopiperazine, cyclo(L-Phe-L-Phe). *Amino Acids*. 1997;12 (1):41-47.
32. Danda H. Essential factors in asymmetric hydrocyanation catalyzed by cyclo (- (R)-Phe-(R)-His-). *Synlett*. 1991;1991(04): 263-264.
33. Tanaka K, Mori A, Inoue S. The cyclic dipeptide cyclo [(S)-phenylalanyl-(S)-histidyl] as a catalyst for asymmetric addition of hydrogen cyanide to aldehydes. *J Org Chem*. 1990;55(1): 181-185.
34. Gdaniec M, Liberek B. Structure of cyclo(-l-phenylalanyl-l-phenylalanyl-). *Acta Crystallograph Sec C-Crystal Struct Commun*. 1986;42:1343-1345.
35. Perez-Mellor A, Zehnacker A. Vibrational circular dichroism of a 2,5-diketopiperazine (DKP) peptide: evidence for dimer formation in cyclo LL or LD diphenylalanine in the solid state. *Chirality*. 2017;29(2):89-96.
36. Garcia AM, Iglesias D, Parisi E, et al. And others. Chirality effects on peptide self-assembly unraveled from molecules to materials. *Chem*. 2018;4(8):1862-1876.
37. Ozawa Y, Sato H, Kayano Y, et al. Self-assembly of tripeptides into c-turn nanostructures. *Phys Chem Chem Phys*. 2019;21(21): 10879-10883.
38. Abo-Riziq AG, Bushnell JE, Crews B, Callahan MP, Grace L, de Vries MS. Discrimination between diastereoisomeric dipeptides by IR-UV double resonance spectroscopy and ab initio calculations. *Int J Quantum Chem*. 2005;105(4):437-445.
39. Pérez Mellor A, Zehnacker A. Chirality effects in jet-cooled cyclic dipeptides. In: Ebata T, Fujii M, eds. *Physical Chemistry of Cold Gas-Phase Functional Molecules and Clusters*. Singapore: Springer; 2019:63-87.
40. Alata I, Perez-Mellor A, Ben Nasr F, et al. Does the residues chirality modify the conformation of a cyclo-dipeptide? Vibrational spectroscopy of protonated cyclo-diphenylalanine in the gas phase. *J Phys Chem A*. 2017;121(38):7130-7138.
41. Dunbar RC, Steill JD, Oomens J. Chirality-induced conformational preferences in peptide-metal ion binding revealed by IR spectroscopy. *J Am Chem Soc*. 2011;133(5):1212-1215.
42. Lepere V, Le Barbu-Debus K, Clavaguera C, et al. Chirality-dependent structuration of protonated or sodiated polyphenylalanines: IRMPD and ion mobility studies. *Phys Chem Chem Phys*. 2016;18(3):1807-1817.
43. Moss J, Bundgaard H. Kinetics and mechanism of the facile cyclization of histidyl-prolineamide to cyclo (his-pro) in aqueous-solution and the competitive influence of human plasma. *J Pharm Pharmacol*. 1990;42(1):7-12.
44. Capasso S, Vergara A, Mazzarella L. Mechanism of 2,5-dioxopiperazine formation. *J Am Chem Soc*. 1998;120(9): 1990-1995.
45. Szardenings AK, Burkoth TS, Lu HH, Tien DW, Campbell DA. A simple procedure for the solid phase synthesis of diketopiperazine and diketomorpholine derivatives. *Tetrahedron*. 1997;53(19):6573-6593.
46. Merten C, Kowalik T, Hartwig A. Vibrational circular dichroism spectroscopy of solid polymer films: effects of sample orientation. *Appl Spectrosc*. 2008;62(8):901-905.
47. Buffeteau T, Lagugne-Labarthe FS, Sourisseau C. Vibrational circular dichroism in general anisotropic thin solid films: measurement and theoretical approach. *Appl Spectrosc*. 2005;59(6): 732-745.
48. Cao XL, Fischer G. Infrared spectra of monomeric L-alanine and L-alanine-N-d(3) zwitterions isolated in a KBr matrix. *Chem Phys*. 2000;255(2-3):195-204.
49. Basiuk VA, Gromovoy TY, Glukhoy AM, Golovaty VG. Chemical-transformations of proteinogenic amino-acids during their sublimation in the presence of silica. *Orig Life Evol Biosph*. 1991;21(3):129-144.
50. Kama AB, Genois R, Massuyeau F, Sidibe M, Diop CAK, Gautier R. Cyclohexylammonium sulfanilate: a simple representative of the chiral materials containing only achiral building units. *Mater Lett*. 2019;241:6-9.
51. Sunatsuki Y, Fujita K, Maruyama H, et al. Chiral crystal structure of a P2(1)2(1)2(1) kryptoracemate iron (II) complex with an unsymmetric azine ligand and the observation of chiral single crystal circular dichroism. *Cryst Growth Des*. 2014;14(8): 3692-3695.
52. Brizard A, Aime C, Labrot T, et al. Counterion, temperature, and time modulation of nanometric chiral ribbons from gemini-tartrate amphiphiles. *J Am Chem Soc*. 2007;129(12): 3754-3762.
53. Chang BS, Li X, Sun TL. Self-assembled chiral materials from achiral components or racemates. *Eur Polym J*. 2019;118: 365-381.
54. Gautier R, Klingsporn JM, Van Duyne RP, Poeppelmeier KR. Optical activity from racemates. *Nat Mater*. 2016;15(6):591-592.
55. Quesada-Moreno MM, Cruz-Cabeza AJ, Aviles-Moreno JR, et al. The curious case of 2-propyl-1H-benzimidazole in the solid state: an experimental and theoretical study. *J Phys Chem A*. 2017;121(30):5665-5674.
56. Asselin P, Madebene B, Soulard P, et al. Competition between inter- and intra-molecular hydrogen bonding: an infrared spectroscopic study of jet-cooled amino-ethanol and its dimer. *J Chem Phys*. 2016;145(22).
57. Oswald S, Seifert NA, Bohle F, et al. The chiral trimer and a metastable chiral dimer of achiral hexafluoroisopropanol: a multi-messenger study. *Angewandte Chemie Int Ed*. 2019;58 (15):5080-5084.
58. Bodansky M. *Principles of Peptides Synthesis*. Berlin: Springer Verlag; 1984.
59. Zhu YY, Tang MS, Shi XY, Zhao YF. Quantum chemical study of cyclic dipeptides. *Int J Quantum Chem*. 2007;107(3):745-753.
60. Xia P, Wang C, Qi C. Theoretical study on the cyclization mechanism of dipeptides. *Chin J Chem*. 2013;31(6):813-818.
61. Frisch MJ, Trucks GW, Schlegel HB, Scuseria GE, Robb MA, Cheeseman JR, Scalmani G, Barone V, Mennucci B, Petersson GA, Nakatsuji H, Caricato M, Li X, Hratchian HP, Izmaylov AF, Bloino J, Zheng G, Sonnenberg JL, Hada M, Ehara M, Toyota K, Fukuda R, Hasegawa J, Ishida M, Nakajima T, Honda Y, Kitao O, Nakai H, Vreven T, Montgomery JA, Peralta JE, Ogliaro F, Bearpark M, Heyd JJ, Brothers E, Kudin KN, Staroverov VN, Kobayashi R, Normand J, Raghavachari K, Rendell A, Burant JC, Iyengar SS,

Tomasi J, Cossi M, Rega N, Millam JM, Klene M, Knox JE, Cross JB, Bakken V, Adamo C, Jaramillo J, Gomperts R, Stratmann RE, Yazyev O, Austin AJ, Cammi R, Pomelli C, Ochterski JW, Martin RL, Morokuma K, Zakrzewski VG, Voth GA, Salvador P, Dannenberg JJ, Dapprich S, Daniels AD, Farkas Ö, Foresman JB, Ortiz JV, Cioslowski J, Fox DJ. Gaussian 09, Revision B.01. 2010.

How to cite this article: Pérez-Mellor A, Le Barbu-Debus K, Zehnacker A. Solid-state synthesis of cyclo LD-diphenylalanine: A chiral phase built from achiral subunits. *Chirality*. 2020;1–12. <https://doi.org/10.1002/chir.23195>

SUPPORTING INFORMATION

Additional supporting information may be found online in the Supporting Information section at the end of this article.